Eur. Phys. J. B **47**, 437–441 (2005)
DOI: 10.1140/epjb/e2005-00334-9

THE EUROPEAN PHYSICAL JOURNAL B

Spin-polarized transport in carbon nanotubes with impurities

H. Pan[1,2,a], T.H. Lin[2], and D. Yu[2]

[1] Department of Physics, Beijing University of Aeronautics and Astronautics, Beijing 100083, P.R. China
[2] State Key Laboratory for Mesoscopic Physics and Department of Physics, Peking University, Beijing 100871, P.R. China

Received 10 February 2005 / Received in final form 27 July 2005
Published online 28 October 2005 –

Abstract. Impurity effects on the spin-polarized transport through armchair carbon nanotubes contacted by ferromagnetic leads are investigated theoretically. The length of the nanotube can cause on-resonance and off-resonance behaviors of the spin-coherent transport. The impurity suppresses the conductance for the on-resonance case, while it enhances the conductance for the off-resonance one. With increasing impurity strength, the tunnel magnetoresistance exhibits a maximum or minimum value for the on-resonance or off-resonance case, respectively.

PACS. 72.25.-b Spin polarized transport – 73.63.-b Electronic transport in nanoscale materials and structures – 73.63.Fg Nanotubes

1 Introduction

The exciting discovery of carbon nanotubes [1] has stimulated a lot of experimental and theoretical studies due to their special geometrical and electronic properties [2]. Perfect carbon nanotubes are predicted to be either metallic or semiconducting depending on their diameter and chirality, which is uniquely determined by the chiral vector (n, m), where n and m are integers [3–5]. Research on electron transport through hybrid device is presented in which nanotubes are coupled to different materials. A carbon-nanotube-based nanodevice is possible when finite nanotubes can be efficiently fabricated and coupled to external leads. Carbon nanotubes are considered as promising spin mediators because of their ballistic conduction nature and long spin scattering length [6–8]. Coherent spin transport has been observed in multi-walled carbon nanotube systems with Co electrodes [6–8]. The spin-dependent transport of a single-walled carbon nanotube contacted with Co electrodes has also been reported experimentally [9]. It has been found that carbon nanotubes show quite a considerable giant magnetoresistance (GMR) effect. Theoretical investigation of the transport properties of these hybrid nanotube devices is of great importance, not only for their basic scientific interest, but also aiming at the design of novel spintronic devices. Carbon nanotubes exhibit different kinds of features in quantum transport. Some show single-electron tunneling behavior, and some show Luttinger liquid behavior, depending on the barrier contact with the external electrodes. Resonant spin polarized currents in the ferromagnetic/carbon-nanotube/ferromagnetic (FM/CNT/FM) system have been studied theoretically, where the single electron model has been used [10]. Recently, spin transport in a one-dimensional quantum wire (carbon nanotube) described by Luttinger liquid theory has also been studied, where strong electron-electron interaction has been included [11].

However, the impurity effects on the system are not considered in most cases. Experimental and theoretical studies have indicated that the electronic and transport properties of carbon nanotubes can be substantially modified by point defects such as vacancies and substitutional impurities [12–15]. Since carbon nanotubes are not strictly one-dimensional (1D) materials but are quasi-1D ones, it is expected that the impurity has unique effects on the system. In this paper, impurity effects on spin-polarized transport in the hybrid FM/CNT/FM system are theoretically studied. In such a system, the tunneling property exhibits special behavior due to the detailed construction and structure of the nanotubes. The energy of the finite-sized carbon nanotubes is quantized both in the longitudinal and transverse directions, which increases the tunneling channels. By using standard nonequilibrium Green's function (NGF) techniques [16–18], we have analyzed the quantum transport properties of the FM/CNT/FM system with impurities. Since the impurity changes the energy structure of the carbon nanotube, it has a great influence on the transport properties of the system.

2 Physical model and formula

The FM/CNT/FM system under consideration can be described by the following Hamiltonian

$$H = \sum_{\alpha=L,R} H_\alpha + H_C + H_T, \tag{1}$$

[a] e-mail: hpan@pku.edu.cn

with

$$H_\alpha = \sum_{k,\sigma} \epsilon_{\alpha,k\sigma} a^\dagger_{\alpha,k\sigma} a_{\alpha,k\sigma} \tag{2}$$

$$H_C = \sum_{n,\sigma} (\epsilon^0_n - e v_g) d^\dagger_{n\sigma} d_{n\sigma},$$

$$H_T = \sum_{n,k\sigma\sigma'} \left[t_L a^\dagger_{L,k\sigma} d_{n\sigma} + \text{h.c.} \right] + \left[t_R \left(\cos\frac{\theta}{2} a^\dagger_{R,k\sigma} d_{n\sigma'} - \sigma \sin\frac{\theta}{2} a^\dagger_{R,k\bar{\sigma}} d_{n\sigma'} \right) + \text{h.c.} \right],$$

where H_α describes the ferromagnetic leads and has already been diagonalized by the Bogliubov transformation [16]. H_C is the Hamiltonian of the central conductor with multiple discrete energy levels ϵ^0_n, since the finite-length carbon nanotubes can be taken as quantum dots. v_g is the gate voltage which controls the energy levels in the carbon nanotube. H_T denotes the tunneling part of the Hamiltonian, and $t_{L,R}$ are the hopping matrix. It is noted that electron-electron interaction is important and can result in Luttinger liquid behavior in carbon nanotubes [11]. Usually power law behavior occurs at a relatively high temperature. The behavior of the system considered here is at a very low temperature. Furthermore, some transport properties in nanotubes can be well explained by using a single-electron model despite possibly important electron-electron interaction effects [10,13,14,19,20]. One can obtain the qualitative understanding of the experimental results observed from a sing-electron picture of the impurity related effects on the electron transport in a CNT. The reason may be that a single-electron description is appropriate when the bias voltage and the temperature are much lower than the energy-level spacing of the experimental sample. Based upon this consideration, the single-electron model is used in this paper. The carbon nanotubes can be well described by the tight-binding model with one π-electron per atom as $H_{tube} = \sum_{\langle i,j\rangle,\sigma} [-\gamma_0 c^\dagger_{i\sigma} c_{j\sigma} + \text{h.c.}] + U c^\dagger_0 c_0$, where i, j are restricted to nearest-neighbor atoms, and the bond potential $\gamma_0 = 2.75$ eV. This model is known to give a reasonable and qualitative description of the electronic and transport properties of carbon nanotubes [10,13,14,19,20]. In this π-electron tight-binding model, the defect-free nanotubes have complete electron-hole symmetry with their Fermi levels at zero [13].

The impurity is defined by setting the site energy equal to U at one of the sites of the unit cell, and various strengths represent typical substitutional impurities or a vacancy. For example, the strength $U = 3$, -5 and 10^6 can simulate substitutional boron, nitrogen, and a vacancy respectively, according to former tight-binding and *ab inito* calculations [14,15]. The discrete energy levels ϵ^0_n can be obtained by numerically diagonalizing H_{tube}. The conductance and current can be calculated from standard NGF techniques. The Green's function can be expressed conveniently by

$$\mathbf{G}^r_n(t,t') = \begin{pmatrix} G^r_{n,\uparrow\uparrow}(t,t') & G^r_{n,\uparrow\downarrow}(t,t') \\ G^r_{n,\downarrow\uparrow}(t,t') & G^r_{n,\downarrow\downarrow}(t,t') \end{pmatrix}, \tag{3}$$

where $G^r_{n,\sigma\sigma'}(t,t') = -i\theta(t-t')\langle\{d_{n,\sigma}(t), d^\dagger_{n,\sigma'}(t')\}\rangle$. By means of the standard NGF technique, the current can be derived as [10,16]

$$I_\alpha = \frac{ie}{\hbar} \int \frac{\mathrm{d}\epsilon}{2\pi} \sum_n Tr_\sigma \{ \mathbf{\Gamma}_\alpha(\epsilon) [\mathbf{G}^<_n(\epsilon) + f_\alpha(\epsilon)(\mathbf{G}^r_n(\epsilon) - \mathbf{G}^a_n(\epsilon))] \}, \tag{4}$$

where $f_\alpha(\epsilon)$ is the Fermi distribution function, and $\mathbf{\Gamma}_\alpha(\epsilon)$ is the linewidth function. Under the wide-bandwidth approximation, the linewidth functions are independent of the energy variables. Furthermore, the linewidth functions are assumed to be independent of the energy levels. This means that the transporting electrons in the leads are equally coupled to different energy levels of the CNT. $\mathbf{G}^r$ and $\mathbf{G}^<$ are the retarded and correlated Green's functions, respectively. They can be calculated from the Dyson equation $\mathbf{G}^r = [(\mathbf{g}^r)^{-1} - \mathbf{\Sigma}^r]^{-1}$ and the Keldysh equation $\mathbf{G}^< = \mathbf{G}^r \mathbf{\Sigma}^< \mathbf{G}^a$. $\mathbf{g}^r$ is the retarded Green's function of the uncoupled nanotube. The selfenergies $\mathbf{\Sigma}^r$ and $\mathbf{\Sigma}^<$ are given as $\mathbf{\Sigma}^r = -\frac{i}{2}(\mathbf{\Gamma}_L + \mathbf{\Gamma}_R)$ and $\mathbf{\Sigma}^< = i(f_L \mathbf{\Gamma}_L + f_R \mathbf{\Gamma}_R)$. The coupling between the CNT and the respective FM leads are given by

$$\mathbf{\Gamma}_L = \begin{pmatrix} \Gamma_{L\uparrow}(1+P_L) & 0 \\ 0 & \Gamma_{L\downarrow}(1-P_L) \end{pmatrix}, \tag{5}$$

and

$$\mathbf{\Gamma}_R = \begin{pmatrix} \Gamma_{R\uparrow}(1+P_R\cos\theta) & \Gamma_{R\uparrow\downarrow} P_R \sin\theta \\ \Gamma_{R\downarrow\uparrow} P_R \sin\theta & \Gamma_{R\downarrow}(1-P_R\cos\theta) \end{pmatrix}, \tag{6}$$

where P_α is the polarization of the αth lead. For the case of two same FM leads, we can take $P = P_L = P_R$, and $\Gamma_{\uparrow(\downarrow)} = \Gamma_{L\uparrow(\downarrow)} = \Gamma_{R\uparrow(\downarrow)}$. Furthermore, we define two parameters as $\eta = \Gamma_\uparrow/\Gamma_\downarrow$ and $\Gamma = \Gamma_\uparrow + \Gamma_\downarrow$. The linewidth functions Γ are set as small values compared with the energy-level spacing for the symmetric and weak-coupling case. In the steady state, the total current is

$$I = \frac{1}{2}(I_L - I_R) = \frac{e}{h} \int \mathrm{d}\epsilon T_{eff}(\epsilon)[f_L(\epsilon) - f_R(\epsilon)], \tag{7}$$

where

$$T_{eff} = \sum_n Tr_\sigma \mathbf{\Gamma}_L \mathbf{G}^r_n(\epsilon) \mathbf{\Gamma}_R \mathbf{G}^a_n(\epsilon). \tag{8}$$

At zero temperature, the conductance can be obtained as: $G = \frac{e^2}{h} T_{eff}$, and the tunnel magnetoresistance (TMR) can be defined as $TMR(\theta) = 1 - G(\theta)/G(0)$. The energy and the nanotube length in the calculations are scaled by γ_0 and the lattice constant $a = 0.245$ nm, respectively. The conductance G is scaled by the unit of quantum conductance $G_0 = 2e^2/h$. The linewidth is set as $\Gamma = 0.02\gamma_0$ for the weak-coupling case. In the following, the numerical

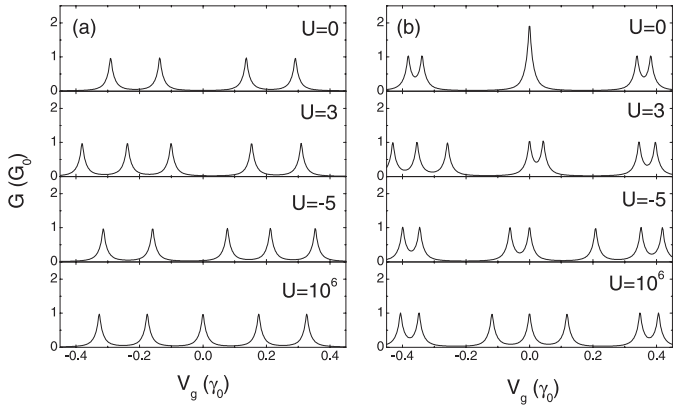

Fig. 1. The conductance G at $\theta = \pi/3$ versus v_g for (6,6) nanotube of length $L = 6$ (a) and $L = 7$ (b) with different U.

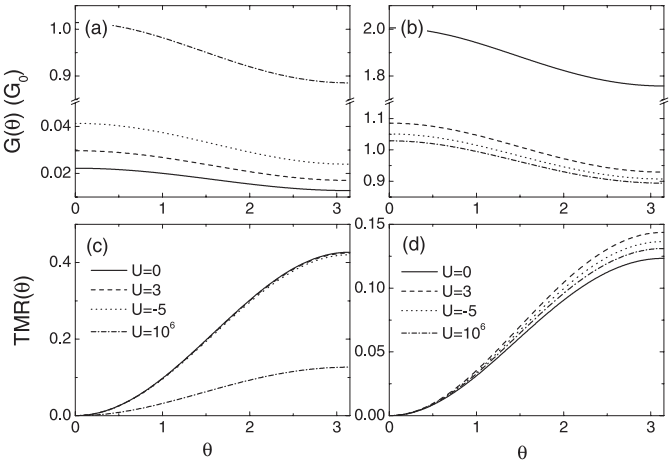

Fig. 2. The conductance G versus θ for (6,6) nanotube of length $L = 6$ (a) and $L = 7$ (b) with different U. (c) and (d) are the corresponding TMR.

results are discussed in detail for the (6,6) armchair nanotube. For armchair nanotubes, the length L is measured in terms of unit cells: a unit cell is the repeat unit along the armchair tube consisting of two carbon rings. The length is selected as $L = 6$ or $L = 7$, which is shorter than the spin coherence length [9]. $\eta = 2$ means that $\Gamma_\uparrow > \Gamma_\downarrow$, and then the tunneling probability of electrons from the spin up subband to spin up subband is less than that from down to down subbands.

3 Results and discussion

To clarify the impurity effects, the conductance $G(\theta = \pi/3)$ vs. V_g at different U are plotted in Figure 1. For nanotubes with $U = 0$, the conductance at the Fermi level $E_F = 0$ is about 0 for $L = 6$ and about $2G_0$ for $L = 7$, respectively. Such a difference is a reflection of the energy structure of the nanotubes with different length, because the resonant states are close to the eigenstates of the corresponding isolated nanotubes at small coupling strength Γ. In general, one resonant state appears at the Fermi level with $L = 3N + 1$ (N denoting the number of the repeating carbon units), because $k_F = 2\pi/3$ is now an allowed wave vector. Large conductance exists at the Fermi level due to the overlap of the π and π^* bands there [21]. For other lengths, k_F is not an allowed wave vector and no resonant state exists at the Fermi level, thus G is much smaller due to the energy gap between the resonant states. The impurity, such as substitutional boron (nitrogen) or a vacancy, in the infinite-length carbon nanotube can lead to a quasibound state near the lower or upper subbands [15]. Similarly, it can induce one resonant state for finite-length carbon nanotubes. As seen from Figure 1, one new resonant state appears below the Fermi level for both $L = 6$ and $L = 7$ at $U = 3$. An impurity with negative strength $U = -5$ has similar effects as the one with positive strength, except that the resonant state induced by the impurity is above the Fermi energy. The resonant state associated with positive or negative U is analogous to the acceptor or donor state in semiconductors [15], which lead to a resonant state below or above the Fermi level, respectively. Since a single impurity breaks the mirror symmetry planes containing the tube axis, the original resonant state at $E_F = 0$ for $L = 7$ is split into two. One of the two states is still at the Fermi level, and the other is above or below the Fermi level according to positive or negative U. Furthermore, the electron-hole symmetry in the perfect nanotubes within the π-band approximation is also broken because the new resonant state is near the Fermi level [13]. The position of the resonant state induced by the impurity is related to the impurity strength [14,15]. With the increase of U, the position of the resonant state induced by the impurity approaches the Fermi level. For the single vacancy with very strong $U = 10^6$, the resonant state induced by the impurity is just located at the Fermi level for both $L = 6$ and $L = 7$, which results in the recovery of the electron-hole symmetry.

Figure 2 shows the dependence of G and TMR at the Fermi level on the magnetic moment orientation θ with different L and U. For both cases of $L = 6$ and $L = 7$, G decreases with increasing θ, which is the well-known result for the TMR junctions at zero bias. G has the largest (smallest) value when the magnetic moment of the left and right leads are parallel (antiparallel). For nanotubes with $L = 6$ and $U = 0$, G is very small and shows off-resonance behaviour. However, G becomes larger if there exists an impurity with $U = 3$ or $U = -5$ in the nanotube. The stronger the impurity, the larger the conductance. The system can even show on-resonance behavior at a very strong $U = 10^6$ with conductance of about one G_0. For nanotubes with $L = 7$ and $U = 0$, G is large and shows on-resonance behavior. Quite different from the case of $L = 6$, G decreases to about one half of the original value if there exists an impurity. The change hardly depends on the impurity strength. As shown in Figures 2c and 2d, the TMR has a minimum value in the parallel configuration and a maximum value in the antiparallel configuration, respectively. The θ dependence of TMR shows a clear spin-valve effect, in agreement with the TMR experimental

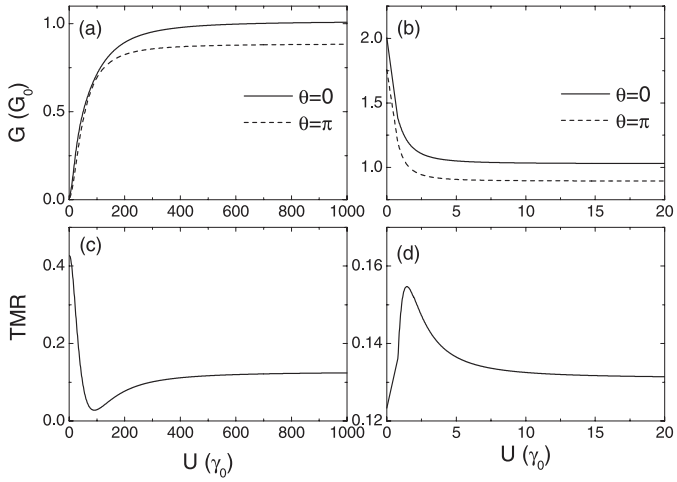

Fig. 3. The conductance G and TMR versus U for (6,6) nanotube of length $L = 6$ (a) and $L = 7$ (b).

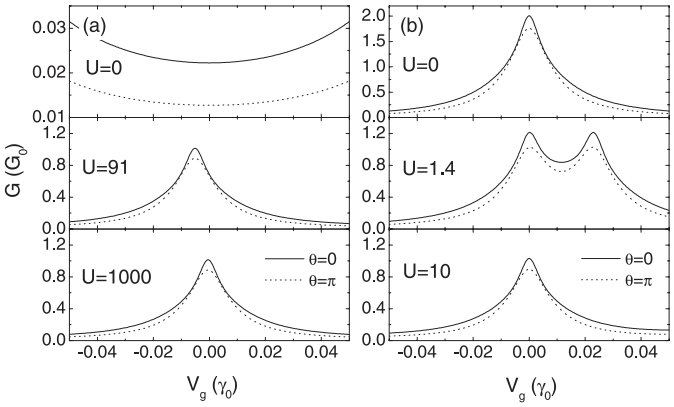

Fig. 4. The conductance G at $\theta = 0$ and $\theta = \pi$ versus v_g for (6,6) nanotube of length $L = 6$ (a) and $L = 7$ (b) with different U.

results [6,7]. For the off-resonance case, the impurity with weak strength has little influence on the *TMR*. Only the impurity with very strong strength can decrease the TMR distinctly because it induces a resonant state at the Fermi level. For the on-resonance case, however, the impurity has much less influence. The *TMR* increases only a little with increasing U, because there still exists one resonant state at the Fermi level despite the impurity.

The dependence of G at the Fermi level and *TMR* on U is plotted in Figure 3 to clearly show the effects of the impurity strength. It is seen that G increases with U and finally reaches a constant of about one G_0 for the nanotube with $L = 6$, because the resonant state induced by the impurity approaches the Fermi level with increasing U. While for the nanotube with $L = 7$, G decreases rapidly from about two G_0 to one G_0 with U, because the original two resonant states at the Fermi level are split and only one is left there due to the impurity. It means that whether the impurity increases or decreases the conductance depends on the nanotube length. For both cases, the conductance at $\theta = 0$ is greater than that at $\theta = \pi$. The TMR for the two cases are quite different as shown in Figures 3c and 3d. The TMR has a minimum value at $U = 91$ for $L = 6$, while it has a maximum value at $U = 1.4$ for $L = 7$. From the definition $TMR = 1.0 - G(\pi)/G(0)$, it is known that a larger ratio $G(\pi)/G(0)$ will result in a smaller TMR.

In order to better understand the minimum and maximum values in the TMR, $G(0)$ and $G(\pi)$ at some typical U for $L = 6$ and $L = 7$ are plotted in Figure 4. Although $G(0)$ and $G(\pi)$ at the Fermi level are very small for the nanotube with $L = 6$ and $U = 0$, the small ratio of $G(\pi)/G(0)$ leads to the large TMR. With increasing U, the peaks of $G(0)$ and $G(\pi)$ approach the Fermi level. During this procedure, the difference between $G(0)$ and $G(\pi)$ at the Fermi level first decreases and then increases, resulting in a maximum of the ratio. Thus a minimum of the TMR appears at $U = 91$. While for the nanotube with $L = 7$ and $U = 0$, $G(0)$ and $G(\pi)$ are very large but with a small difference between their values at the Fermi level, resulting in a large ratio and small TMR. With increasing U, the original resonant state is split into two as mentioned above. During this procedure, the difference between $G(0)$ and $G(\pi)$ at the Fermi level first increase and then decrease, resulting in a minimum of the ratio. Thus a maximum of the TMR appears at $U = 1.4$.

4 Conclusion

In summary, we have investigated impurity effects on spin-polarized transport in the FM/CNT/FM system theoretically. The system shows on-resonance behavior for the perfect armchair carbon nanotube with length $L = 3N + 1$ and shows off-resonance behavior with other lengths. The impurity suppresses conductance for the on-resonance case, while it enhances the conductance for the off-resonance case. The impurity induces one new resonant state whose position depends on the impurity strength. When the impurity is near the Fermi level, the electron-hole symmetry can be broken. While for very high impurity strengths, the resonant state is just located at the Fermi level, which results in recovery of the electron-hole symmetry. Furthermore, the impurity strength has a more distinct influence on conductance for the on-resonance case than for the off-resonance one. With increasing impurity strength, the *TMR* has a maximum value for the on-resonance case, while it has a minimum value for the off-resonance one, respectively.

This project is supported by NSFC under Grants No. 90103027 and No. 50025206, and the National "973" Projects Foundation of China (No. 2002CB613505).

References

1. S. Iijima, Nature (London) **354**, 56 (1991)
2. R. Saito, G. Dresselhaus, M.S. Dresselhars, *Physical Properties of Carbon Nanotubes* (Imperial College Press, London, 1998)

3. J.W. Mintmire, B.I. Dunlap, C.T. White, Phys. Rev. Lett. **68**, 631 (1992)
4. N. Hamada, S.I. Sawada, A. Oshiyama, Phys. Rev. Lett. **68**, 1579 (1992)
5. R. Saito, M. Fujita, G. Dresselhaus, M.S. Dresselhars, Appl. Phys. Lett. **60**, 2204 (1992)
6. K. Tsukagoshi, B.W. Alphenaar, H. Ago, Nature (London) **401**, 572 (1999)
7. B.W. Alphenaar, K. Tsukagoshi, M. Wagner, J. Appl. Phys. **89**, 6863 (2001)
8. B. Zhao, I. Monch, H. Vinzelberg, T. Muhl, C.M. Schneider, Appl. Phys. Lett. **80**, 3144 (2002)
9. J.R. Kim, H.M. So, J.J. Kim, Phys. Rev. B **66**, 233401 (2002)
10. H. Mehrez, J. Taylor, H. Guo, J. Wang, C. Roland, Phys. Rev. Lett. **84**, 2682 (2000)
11. L. Balents, R. Egger, Phys. Rev. Lett. **85**, 3464 (2000); L. Balents, R. Egger, Phys. Rev. B **64**, 035310 (2001)
12. M. Bockrath, W. Liang, D. Bozovic, J.H. Hafner, C.H. Lieber, M. Tinkham, H. Park, Science **291**, 283 (2001)
13. L. Chico, L.X. Benedict, S.G. Louie, M.L. Cohen, Phys. Rev. B **54**, 2600 (1996); L. Chico, V.H. Crespi, L.X. Benedict, S.G. Louie, M.L. Cohen, Phys. Rev. Lett. **76**, 971 (1996); L. Chico, M.P.L. Sancho, M.C. Munoz, Phys. Rev. Lett. **81**, 1278 (1998)
14. T. Kostyrko, M. Bartkowiak, G.D. Mahan, Phys. Rev. B **59**, 3241 (1999)
15. H.J. Choi, J. Ihm, S.G. Louie, M.L. Cohen, Phys. Rev. Lett. **84**, 2917 (2000); H.J. Choi, J. Ihm, Solid State Commun. **111**, 385 (1999)
16. B. Wang, J. Wang, H. Guo, e-print: `arXiv: cond-mat/9910315`
17. Q.F. Sun, T.H. Lin, J. Phys: Condens. Matter **9**, 4875 (1997)
18. H. Pan, T.H. Lin, D. Yu, Phys. Rev. B **70**, 245412 (2004); H. Pan, T.H. Lin, D. Yu, Phys. Lett. A **331**, 231 (2004)
19. M.B. Nardelli, Phys. Rev. B **60**, 7828 (1999)
20. M.B. Nardelli, J. Bernholc, Phys. Rev. B **60**, 16338 (1999)
21. D. Orlikowski, H. Mehrez, J. Taylor, H. Guo, J. Wang, C. Roland, Phys. Rev. B **63**, 155412 (2001)